EXPERIMENTAL STUDY OF SCALED T CROSS-SECTION BEAMS SUBJECTED TO IMPACT LOAD

Oshiro, Roberto E., roberto.oshiro@gmsie.usp.br
Calle, Miguel A.G., miguel.calle@gmsie.usp.br
Mazzariol, Leonardo M., leonardo.mazzariol@gmsie.usp.br
Alves, Marcilio, maralves@usp.br
Group of Solid Mechanics and Structural Impact
Department of Mecatronics and Mechanical Systems Engineering, Polytechnic School, University of São Paulo, São Paulo

Abstract. *It is reported here the experiments of scaled T cross-section beams subjected to transversal impact load. The full-size structure (prototype) is four times larger than the scaled specimen (model), and it will be shown that when the usual scaling laws are applied, the model behaves differently from the prototype when dynamically loaded. In order to compensate for this distortion of similarity, the initial impact velocity is changed in a rational way, leading to a model response similar to the prototype. Quasi-static tests are also carried out so as to compare the static and dynamic behaviour of the scaled structure. It is also discussed here the implications of the scaled structure and the prototype to be made of different materials.*

Keywords*: scaling, similarity, impact*

1. INTRODUCTION

Impact tests carried out on real size structures (prototype) can be very expensive and time consuming when dealing with large compounds such as airplanes, ships, trains, bridges, towers, etc. Accordingly, scaled specimens (models or replicas) can be employed to study the corresponding prototype behaviour. The technique of reproducing the structure response in different scales is termed similarity or similitude, and it has been analysed in many works (Booth et al., 1983; Gregory, 1995; Hu, 2000; Jiang et al., 2006; Li and Jones, 2000; Mazzariol et al., 2010; Me-Bar, 1997; Neuberger et al., 2007; Oshiro and Alves, 2004; Schleyer et al., 2004).

In the case of structural impact, if prototype and model are made of the same material, the factors of the phenomenon can be expressed as a function of the scaling factor, $\beta = L_{\text{model}}/L_{\text{prototype}}$, being L a geometric dimension of the structure. The main relations for the problem of collision of structures are recapitulated in Tab. 1 (Baker et al., 1991; Fox and McDonald, 1998; Murphy, 1950; Jones, 1997; Skoglund, 1967; Szirtes, 1997). In the present work, the model which uses the factors described in Tab. 1 will be referred to as MLT since these factors are derived from the dimensional analysis based on the usual MLT (mass-length-time) basis.

Table 1. Scaling factors relating the main structural model variables to the prototype ones. Factors obtained from the usual scaling laws (MLT).

variable	factor	variable	factor
length, L	β	time, t	β
displacement, δ	β	velocity, V	1
mass, G	β^3	strain rate, $\dot{\varepsilon}$	$1/\beta$
strain, ε	1	acceleration, A	$1/\beta$
stress, σ	1	energy, E'	β^3
force, F	β^2		

However, some structures subjected to dynamic loads do not comply with the usual scaling laws, Tab. 1. Some of the effects that can contribute with this distortion are material strain rate sensitivity, material failure, gravity, etc. When the model behaviour is different of the prototype one, the similarity is named imperfect. Many works reported this problem. Booth et al. (1983) performed drop tests on one-quarter scale to full-scale thin plated mild steel and stainless steel structures. The tests revealed that weld fracture and tearing were considerably more pronounced in the prototype specimens than in the smaller ones. It was also noticed that the prototype reached about 2.5 times the deformation of the 1/4 model at analogous points. Another sample is the work of Schleyer et al. (2004). They analysed the scaling of some mild steel square plates with different edge restrains subjected to uniformly distributed triangular pressure pulse loading. Large inelastic deformations were produced, but no tearing or rupture was noticed. The study observed that the transient response of the plates exhibits some divergence from the laws of geometrically similar scaling. Drazetic et al. (1994) conducted a numerical and experimental study on the scaling of a beam under transverse impact. The scaled

models exhibited some small imperfections, i.e. initial velocity, geometry, and material properties did not strictly follow the linear scaling laws. In order to take these aspects into account, a technique termed non-direct similitude was applied. After correction, the final deformed shape of the model and prototype could be directly compared. Snyman (2010) studied the scaling technique applied to various blast loading experiments. The analysis indicated the importance of material properties such as yield strength and strain rate sensitivity. The author also reported different material properties for the plates used in the tests, although they were made of the same material. This issue is also noticed in the present work.

One of the most prominent features that contribute to the distortion of the scaling laws is the strain rate, $\dot{\varepsilon}$, which may affect the material yielding stress. This behaviour is not predicted by the usual scaling laws, as it can be noticed in Tab. 1, $\beta_\sigma = 1$. In order to take this effect into account, Oshiro and Alves (2009) presented a technique that compensates for the $\dot{\varepsilon}$ effect in scaled structures. Instead of using a single scaling factor, β, a factor for the initial impact velocity, β_V, was employed. One important characteristic of this method is that the factor β_V is calculated without a priori knowledge of the structure response; it relies only on the material properties. A similar approach as presented by Oshiro and Alves (2009) is here applied, as outlined in section 2. The tests setup and material characterization are detailed in section 3, with the main results summarized in section 4. Section 5 discusses the main findings of this investigation, and section 6 closes the paper with the main conclusions.

2. SCALING FACTORS

As previously mentioned, a scaled structure made of a strain rate sensitive material does not comply with the standard similarity laws. Moreover, the sheets used in the tests exhibited different material properties, as will be shown in section 3. Therefore, an adaptation of the method delineated in Oshiro and Alves (2009) is developed in the present work. Instead of the relations presented in Tab. 1, a new set of factors between model and prototype variables are generated. They are valid for models whose material is assumed to be rigid perfectly plastic, and the dynamic yielding stress, σ_d, given by the Norton equation (Lemaitre and Chaboche, 1991),

$$\sigma_\mathrm{d} = \sigma_0 \left(\dot{\varepsilon} / \dot{\varepsilon}_0 \right)^q , \tag{1}$$

q being a material constant and σ_0, the static yielding stress at a strain rate of reference, $\dot{\varepsilon}_0$.

As a means to calculate the factors, a basis comprised by impact velocity, V_0, dynamic yielding stress, σ_d, and impact mass, G, is used to generate the dimensionless numbers (Oshiro and Alves, 2009)

$$\underbrace{\left[\frac{\delta^3 \sigma_\mathrm{d}}{G V_0^2}\right]}_{\Pi_1}, \underbrace{\left[\frac{\dot{\varepsilon}^3 G}{\sigma_\mathrm{d} V_0}\right]}_{\Pi_2}, \underbrace{\left[\frac{A^3 G}{V_0^4 \sigma_\mathrm{d}}\right]}_{\Pi_3}, \underbrace{\left[\frac{t^3 \sigma_\mathrm{d} V_0}{G}\right]}_{\Pi_4}, \underbrace{\left[\frac{\sigma}{\sigma_\mathrm{d}}\right]}_{\Pi_5}, \underbrace{\left[\frac{F^3}{V_0^4 \sigma_\mathrm{d} G^2}\right]}_{\Pi_6}, \underbrace{\left[\frac{E'}{G V_0^2}\right]}_{\Pi_7}, \tag{2}$$

standing δ for displacement, $\dot{\varepsilon}$ for strain rate, A for acceleration, t for time, σ for stress, F for force, and E' for energy.

From the dimensionless numbers Π_1 and Π_2, the factors for dynamic yielding stress, $\beta_{\sigma_\mathrm{d}} = \sigma_\mathrm{dm} / \sigma_\mathrm{dp}$, and strain rate, $\beta_{\dot{\varepsilon}} = \dot{\varepsilon}_\mathrm{m} / \dot{\varepsilon}_\mathrm{p}$, are generated

$$\Pi_{1\mathrm{m}} = \Pi_{1\mathrm{p}} \rightarrow \frac{\beta_\delta^3 \beta_{\sigma_\mathrm{d}}}{\beta_G \beta_V^2} = 1 \rightarrow \beta_{\sigma_\mathrm{d}} = \beta_V^2 \tag{3}$$

and

$$\Pi_{2\mathrm{m}} = \Pi_{2\mathrm{p}} \rightarrow \beta_{\dot{\varepsilon}} \left(\frac{\beta_G}{\beta_{\sigma_\mathrm{d}} \beta_V} \right)^{1/3} = 1 \rightarrow \beta_{\dot{\varepsilon}} = \beta_V / \beta , \tag{4}$$

referring the subscript m to the model and p to the prototype.

In section 3, it will be seen that even though the structures of model and prototype are made of the same material, the quasi-static yielding stress, σ_0, is different. Therefore, the very definition of $\beta_{\sigma_\mathrm{d}}$ provides

$$\beta_{\sigma_\mathrm{d}} = \frac{\sigma_\mathrm{dm}}{\sigma_\mathrm{dp}} = \frac{\sigma_{0\mathrm{m}} \left(\dot{\varepsilon}_\mathrm{m} / \dot{\varepsilon}_0 \right)^q}{\sigma_{0\mathrm{p}} \left(\dot{\varepsilon}_\mathrm{p} / \dot{\varepsilon}_0 \right)^q} = \beta_{\sigma_0} \left(\frac{\dot{\varepsilon}_\mathrm{m}}{\dot{\varepsilon}_\mathrm{p}} \right)^q = \beta_{\sigma_0} \left(\beta_{\dot{\varepsilon}} \right)^q , \tag{5}$$

being $\beta_{\sigma_0} = \sigma_{0\mathrm{m}}/\sigma_{0\mathrm{p}}$.

By inserting Eq. (4) into Eq. (5), it follows that

$$\beta_{\sigma_0} = \beta_{\sigma_0}\left(\beta_V/\beta\right)^q, \tag{6}$$

which, together with Eq. (3) provides

$$\beta_V = \left(\beta_{\sigma_0}\beta^{-q}\right)^{1/(2-q)}. \tag{7}$$

Equation (7) is the impact velocity factor that takes $\beta_{\sigma_0} \neq 1$ and strain rate in a scaled structure into consideration. As a result of this modification, a new set of factors is generated by developing the dimensionless numbers Π_2 to Π_7 and applying Eq. (6) and (7); they are summarized in Tab. 2. A model based on the relations of Tab. 2 will be referred to as VSG-m. It can be noticed that in the case of $\beta_{\sigma_0} = 1$ (identical material), the factors of Tab. 2 are reduced to those developed in Oshiro and Alves. In the case of $q = 0$ (strain rate insensitive material), Tab. 2 is equal to Tab. 1.

Table 2. Scaling factors relating the main structural model variables to the prototype ones. The structure is made of strain rate sensitive material, and $\beta_{\sigma_0} \neq 1$ (VSG-m).

variable	factor	variable	factor
length, L	β	time, t	$\left[\beta_{\sigma_0}{}^{-1}\beta^2\right]^{1/(2-q)}$
displacement, δ	β	velocity, V	$\left[\beta_{\sigma_0}\beta^{-q}\right]^{1/(2-q)}$
mass, G	β^3	strain rate, $\dot{\varepsilon}$	$\left[\beta_{\sigma_0}\beta^{-2}\right]^{1/(2-q)}$
strain, ε	1	acceleration, A	$\left[\beta_{\sigma_0}{}^2\beta^{-q-2}\right]^{1/(2-q)}$
stress, σ	$\left[\beta_{\sigma_0}\beta^{-q}\right]^{2/(2-q)}$	energy, E'	$\left[\beta_{\sigma_0}{}^2\beta^{6-5q}\right]^{1/(2-q)}$
force, F	$\left[\beta_{\sigma_0}\beta^{2(1-q)}\right]^{2/(2-q)}$		

3. EXPERIMENTAL SETUP AND MATERIAL CHARACTERIZATION

3.1. TENSILE TESTS

Low carbon steel 1006 was used to manufacture the T cross-section beams. The reference structure (prototype) was made with a 1.00 mm thick sheet, whereas the model used a 0.25 mm thick sheet – a scaling factor of 1/4. The material stress-strain curve was measured via standard tensile tests, ASTM sheet-type rectangular tension test (ASTM E8). For low velocities, an Instron 3369 testing machine was used with strain rates ranging from 0.00001 s^{-1} to 0.05 s^{-1}. As it can be seen in Fig. 1 (a), although the material of the sheets is nominally the same, the 0.25 mm one is significantly sturdier. The continuous line presents the response of the 1.00 mm thick specimen, and the dotted line is the 0.25 mm specimen. The pointed line shows the 0.25 mm curve adjusted by a factor of $1/\beta_{\sigma_0} = 0.8212$, being $\beta_{\sigma_0} = \sigma_{0\mathrm{m}}/\sigma_{0\mathrm{p}}$. This relation, as shown in section 2, is required to calculate the velocity factor which relates model to prototype.

In order to corroborate the curves obtained in the tensile test, a digital image correlation (DIC) was employed to acquire the strain data. A sequence of 167 images was captured along the entire test using a Nikon D90 camera; one photo taken every 50 s at 12.3 MP resolution and 12 bits colour depth. True strain and instantaneous area values were measured near the neck by analysing a 10 mm x 40 mm area with 2500 quadrilateral elements, Fig. 1 (b). The results confirmed the exponential form, previously assumed for the stress-strain plastic curve of the 1006 steel, for true strain values up to 60.8%, when the specimen presented failure.

The material parameters obtained in the quasi-static tests are: elastic modulus, 200 GPa, hardening modulus, 402 MPa, and quasi-static yielding stress, 168 MPa (for the 1.00 mm thick sheet) and 220 MPa (0.25 mm thick sheet). The factor β_{σ_0} = 1.2177 was determined by adjusting the $\sigma_{\mathrm{true}} - \varepsilon_{\mathrm{true}}$ curve of the 0.25 mm thick sheet to the response of the 1.00 mm thick sheet specimen, Fig. 1 (a). Mass density of the material is 7850 kg/m^3.

3.2. MATERIAL STRAIN RATE PARAMETERS

A split Hopkinson pressure bar was used to obtain the properties of the material at high values of strain rate. Discs of 6 mm diameter and 1 mm thick were employed in the tests, and the strain rate ranged from 3000 s^{-1} to 9000 s^{-1}. The

data obtained from the tests are shown in Fig. 2 (a), being the points gathered on the left side generated by tests at low velocities (Instron testing machine), and the points on far right were obtained from the split Hopkinson bar.

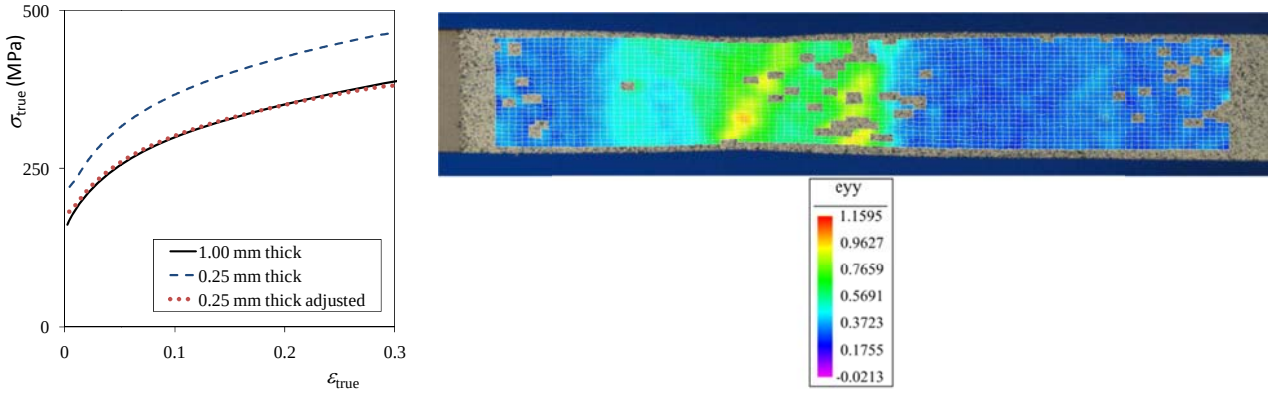

(a) (b)

Figure 1. Characterization of the material at low strain rates. (a) True stress, σ_{true}, as a function of true strain, ε_{true} – curves obtained from tensile tests at $\dot{\varepsilon} = 1E\text{-}5\ s^{-1}$. (b) Strain of the specimen analysed by DIC.

The points of both tests were used to determine the material parameters for strain rate. However, the exponential form of Norton constitutive equation generated a significant deviation from the experimental points. Hence, the Cowper-Symonds relation (Jones, 1997),

$$\sigma_d/\sigma_0 = 1+\left(\dot{\varepsilon}/D\right)^{1/p}, \tag{8}$$

was used to fit the points instead, being D and p material parameters. For the studied case, $D = 4075\ s^{-1}$ and $p = 4.99$, were obtained, Fig. 2 (a). Next, a more suitable range of strain rate for the phenomenon being studied, $0.01\ s^{-1}$ to $800\ s^{-1}$, was chosen, and Eq. (8) was constructed in this region with the constants calculated (continuous line in Fig. 2 (b)). Subsequently, Norton parameters were calculated in order to fit the Cowper-Symonds curve in this region. As a result, the parameters $q = 0.04051$ and $\dot{\varepsilon}_0 = 0.006372\ s^{-1}$ were determined (traced line in Fig. 2 (b)). The range of strain rate is important to define the material parameters (Johnson, 1972).

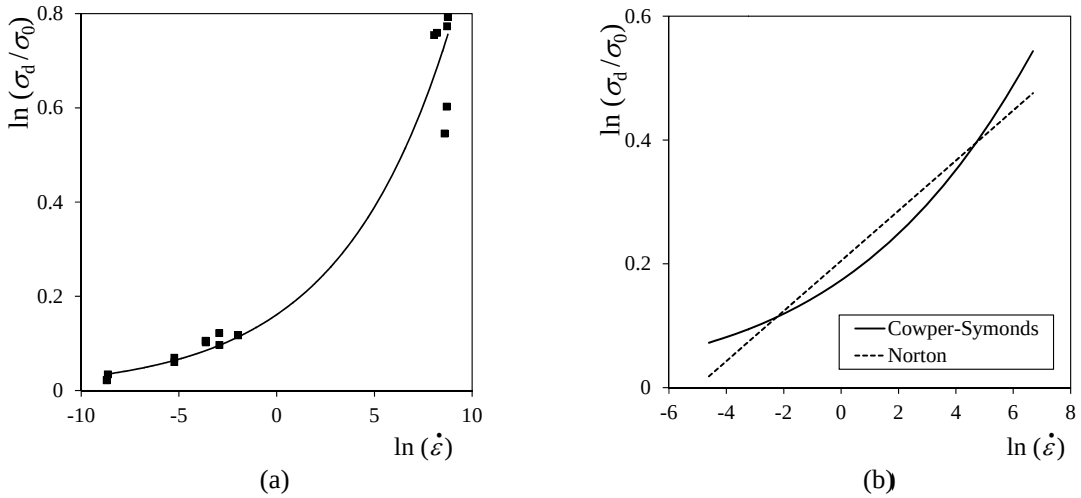

(a) (b)

Figure 2. Fitting of the dynamic yielding stress parameters of the material. (a) Cowper-Symonds parameters fitting to the quasi-static and high strain rate data tests. (b) Norton equation fitting to the Cowper-Symonds constitutive model for strain rate ranging from $0.01\ s^{-1}$ to $800\ s^{-1}$.

3.3. IMPACT TESTS SETUP

The specimen dimensions are presented in Fig. 3: the prototype is made of a 1.00 mm thick mild steel sheet, and the model is composed by a 0.25 mm thick sheet ($\beta = 1/4$). The structure is a T cross-section beam clamped at both ends.

The vertical reinforcement of the structure was welded onto the central line of the top part by a laser process, generating a fillet welding of approximately 0.7 mm (prototype) and 0.3 mm (model).

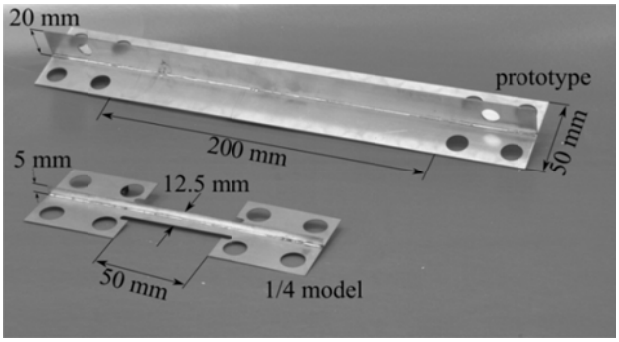

Figure 3. Dimensions of the specimens employed in the impact tests. Prototype made of 1.00 mm thick sheet, and model of 0.25 mm thick sheet.

Since the impact masses employed in the model and prototype exhibited distinct orders of magnitude: 15 kg (prototype) and 0.234 kg (model), two distinct setups were necessary to perform the drop tests, Fig. 4. Linear guide rails with ball slides were used to reproduce a free drop mass. Only vertical displacement was allowed. The indenter was clamped to the ball slides and struck the beam at its mid span. The indenter velocity was measured by a Polytec laser Doppler vibrometer with controller model OFV-3020 and laser model OFV-323.

The indenter was set to hit the specimen slight out of the centreline – the plan of the vertical reinforcement –, so assuring the same collapse mode for all dynamic tests. As a result, the crossed wrinkles configuration did not take place. The wrinkles occurred at the same side of the vertical reinforcement for all the dynamic experiments. This issue is further analysed in section 4.

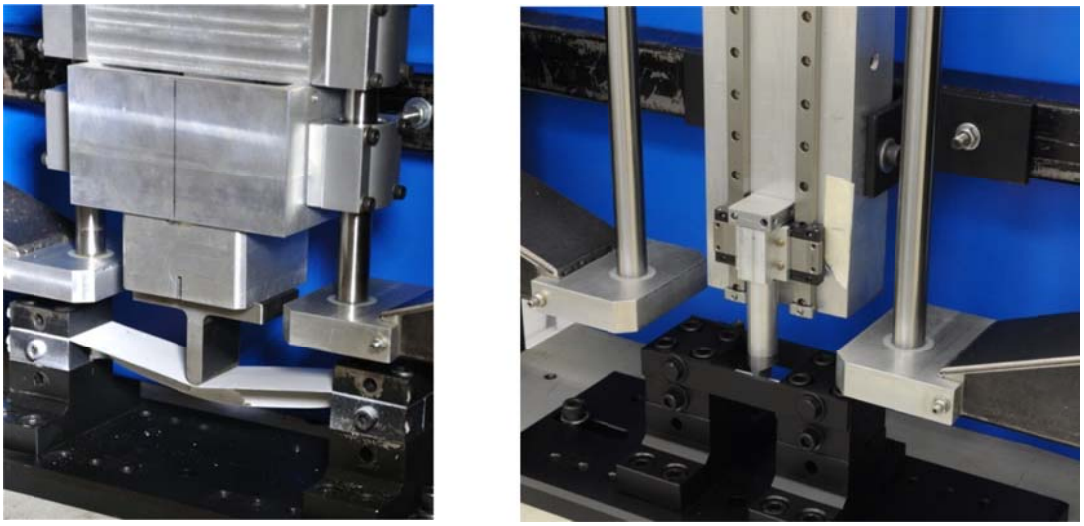

(a) (b)

Figure 4. Setup configuration for the impact tests. (a) Setup for the prototype. (b) Setup for the 1/4 model.

4. RESULTS

4.1. QUASI-STATIC TESTS

Initially, the tests were performed in quasi-static loading by using the Instron testing machine. By so doing, it was possible to compare the response of the model to the real size structure without the effect of strain rate. The VSG-m factors (Tab. 2) with $\beta_{\sigma_0} = 1.2177$ and $q = 0$, were used to transform the model force, $\beta_F = F_m / F_p = \beta_{\sigma_0} \beta^2$. As it can be seen in Fig. 5 (a), the curves of the prototype and the model comported quite similar up to 7 mm of displacement; it started to diverge for higher values of δ, though. This behaviour is explained by the distinct collapse mode that took place in the vertical reinforcement for the model, Fig. 5 (b) and (c). The crossed collapse mode presented by the 1/4 scaled structure absorbs more energy than the mode presented by the prototype.

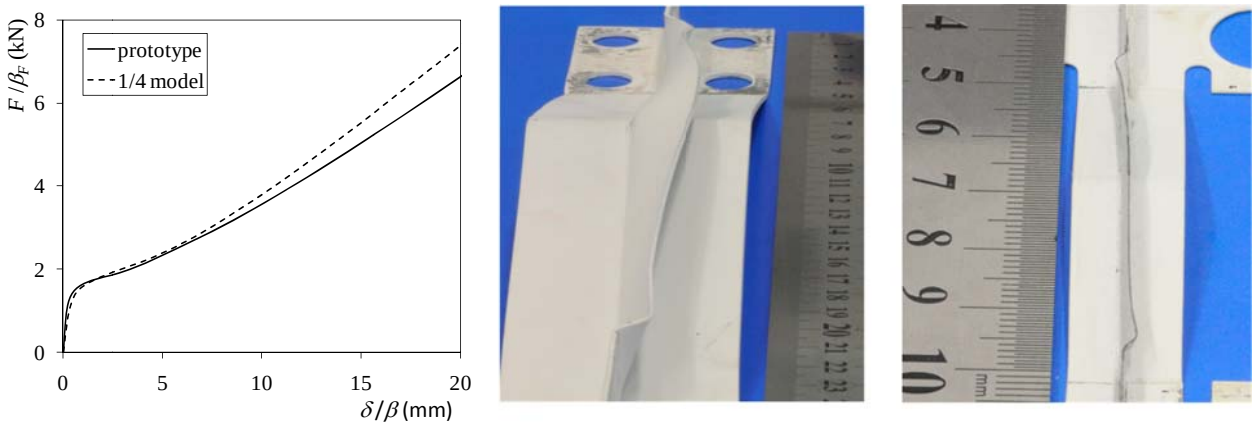

(a) (b) (c)

Figure 5. Results for the beam subjected to quasi-static loading. (a) Reaction force as a function of vertical displacement. (b) Final configuration of deformation of the prototype. (c) Final configuration of the model (crossed wrinkles mode).

4.2. DROP TESTS

Drop tests were performed with the configurations presented in Tab. 3. The results are shown in Fig. 6 with the signal of the laser being integrated to generate the displacement curve and derived to calculate the indenter acceleration. The response of the models was transformed in order to be directly compared to the prototype behaviour. MLT applied the factors of Tab. 1, and VSG-m used Tab. 2. For instance, when comparing the indenter vertical displacement of the prototype to the MLT response, the difference is 15.54%, whereas the VSG-m deviation for the same variable is 0.09%. The difference in reaction force is reduced from 15.02% (MLT) to 4.73% (VSG-m). Total time of the phenomenon can be calculated through the kinetic energy (when it reaches the minimum value). In this case, MLT took 7.72 ms, whereas the VSG-m and the prototype lasted 8.83 ms and 8.92 ms, respectively.

Figure 7 shows the final deformed configuration: (a) prototype and (b) models. The vertical displacement after the impact was measured at the local where the indenter hit the structure. It was computed a displacement of 15.25 mm for the prototype, whilst the MLT and the VSG-m presented 3.15 mm and 3.45 mm, respectively. It corresponds to $\delta =$ 12.60 mm (MLT) and $\delta = 13.80$ mm (VSG-m) after the corresponding scaling factor is applied. Figure 7 also substantiates that the wrinkles in the vertical reinforcement took place at the same side in all experiments, so that they can be compared.

Table 3. Configuration for the impact tests.

	β	β_G	G (kg)	β_V (analytical)	β_V (experimental)	V_0 experimental (m/s)
prototype	1	1	15.68	1	1	3.0592
MLT	1/4	0.0156	0.245	1	0.9841	3.0106
VSG-m	1/4	0.0156	0.245	1.1379	1.1286	3.4526

5. DISCUSSION

Although the structure studied is rather simple, it is suitable to analyse the problem of scaled structures subjected to impact loads. Two features of the scaling laws were examined in the present work by means of real tests: material distortion and imperfect similarity due to strain rate.

Material: in spite of the fact that the similarity laws considers only rigid perfectly plastic material, the present work used material with elastic modulus, 200 GPa, and significant value of hardening, 402 MPa. As a result, the scaling method is an approach for the problem studied. A different methodology could be adopted: a quasi-static average flow stress defined by

$$\sigma_0' = \left[\int \sigma_y(\varepsilon)\mathrm{d}\varepsilon\right] \Big/ \varepsilon \,, \tag{9}$$

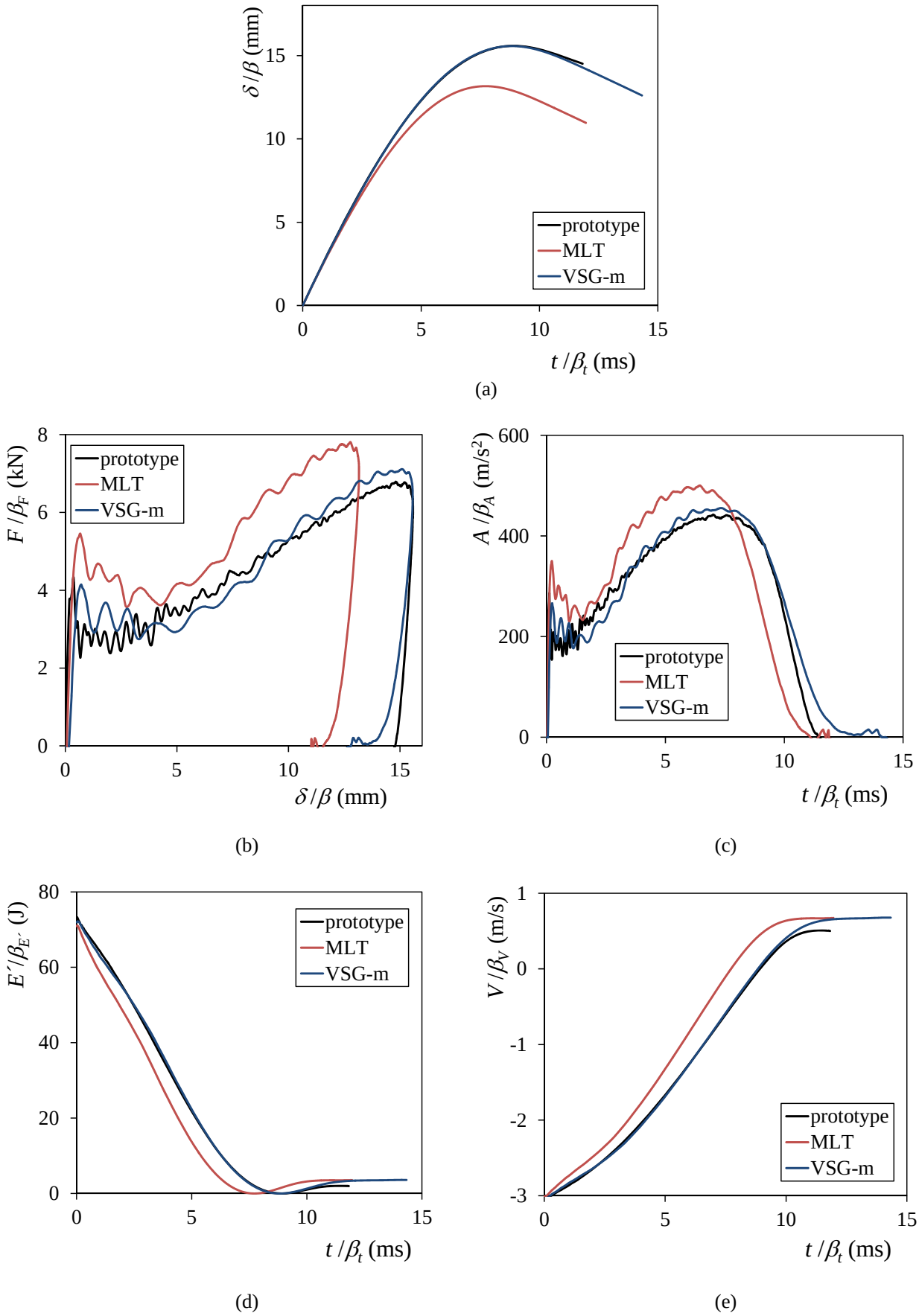

Figure 6. Results of the experimental impact tests. (a) indenter displacement. (b) reaction force. (c) indenter acceleration. (d) total kinetic energy. (e) indenter velocity.

being σ_y the flow stress. In this case, hardening is zero. Furthermore, Fig. 1 shows that the quasi-static yielding stress of model and the real size structure are different ($\sigma_{0m}/\sigma_{0p} = 1.2177$). In order to deal with this shortcoming, the velocity factor was changed so that the kinetic energy compensated for this material feature, Eq. (7) and Tab. 2. Structures made of materials with different properties are frequent in real collision tests, as reported also by Drazetic et al. (1994) and Snyman (2010).

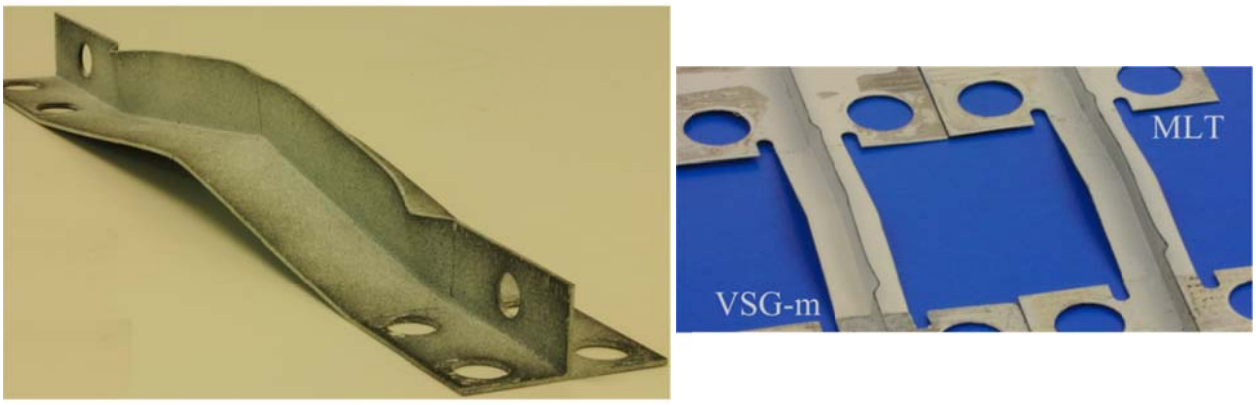

(a) (b)

Figure 7. Final configuration of deformation for the specimens tested with dynamic loads. (a) prototype. (b) MLT and VSG-m.

Strain rate effect: the increase of the dynamic yielding stress due to strain rate was taken into account through the velocity factor, Eq. (7). The Norton constitutive model, Eq. (1), allowed calculating β_V without prior knowledge of the structure response; only the material parameter, q, and the scaling factor, β, were required. Although this effect was less significant than the material dissimilarity – the difference in the quasi-static yielding stress overruled the velocity factor pattern –, it can be more representative for problems in which the models present smaller values of β or higher q.

Quasi-static tests: in the experiments performed in the Instron machine, the force–displacement curve of the model was close to the early response of the prototype. It started to diverge when the material unloading and the crossed wrinkles mode (Fig. 5) took place, though. The initial phase of this test served to corroborate the perfect similarity for the MLT when the dynamic effects are negligible.

After the tests, no failure was detected on the welding fillet of the specimens. However, a small sliding of the specimens relatively to the supports was noticed. In addition, the supports presented horizontal deflection towards the centre when the beam was loaded. This horizontal displacement was monitored during the quasi-static tests with dial depth gages. The maximum value registered was 0.185 mm and 0.135 mm on the right and left side, respectively. Nevertheless, these values are negligible when compared to the corresponding vertical displacement of the beam (30 mm).

Dynamic tests: the dynamic effect can be checked comparing the force magnitude in Fig. 6 (b) with the curve in Fig. 5 (a), the former exhibits a significant increase. For example, the prototype in quasi-static test presented a reaction force of 3.57 kN for 10 mm displacement, whereas the corresponding value for the dynamic test increased to 5.31 kN. Additionally, the curves in the dynamic loading exhibit an initial peak force that is non-existent in the quasi-static case, Fig. 5 (a).

When comparing the models to the real-size structure, the behaviour of the VSG-m is closer to the prototype than the MLT, as it can be seen in Fig. 6 (a) to (e). The values of vertical maximum displacement, δ_{max}, indenter maximum acceleration, A_{max}, maximum reaction force, F_{max}, average force acting on the structure, $F_{average}$, and total time of the impact, t_{total}, are compared in Tab. 4. Nevertheless, as it can be noticed in Tab. 3, the value of impact velocity was slight different from the β_V required by the similarity method, $V_0 = 3.4137$ m/s. MLT presented β_V = 0.9841 (1.59% error), and VSG-m, β_V = 1.1286 (0.82% error). This difference is explained by the difficulty in controlling more accurately the velocity impact during the experiments. However, this deviation is negligible as substantiated by the results.

Method limitations: in the dynamic tests, the VSG-m and MLT presented the same collapse mode of the prototype (Fig.

7), hence it was possible to evaluate the results. If dissimilar deformation were developed, the responses could not be compared since they represent different phenomena. The method studied in the present work compensates for the strengthening of the material due to strain rate and discrepancy in σ_0 by changing the kinetic energy, i.e. it corrects the global response of the structure. Consequently, it can be applied to structures whose collapse configuration is always the same. Also, an analysis of Fig. 6 (a) shows that the vertical displacement of VSG-m follows the behaviour of the prototype up to the maximum value, but after that, these curves started to present a slight divergence. It is explained by the elastic part of the material: since this feature was not contemplated in the method, some difference commenced to take place with the material elastic recovery during the unloading.

Table 4. Results for the experimental tests.

	δ_{max} (mm)	A_{max} (m/s^2)	F_{max} (kN)	$F_{average}$ (kN)	t_{total} (ms)
prototype	15.58	442.33	6.79	5.25	8.92
MLT	13.16	500.43	7.81	6.10	7.72
VSG-m	15.57	455.37	7.11	5.39	8.83

Comparison with previous works: some of the data here generated can be compared with the results of Mazzariol et al. (2010). They tested experimentally the same structure of 1 mm thickness and extrapolated the results to a 20 times larger prototype by using numerical simulations. The strengthening of the material due to strain rate effect was considered by changing the impact mass – instead of the impact velocity as done in the present work. A representative consistency between the results can be observed after the transformation factors are accordingly applied to the data generated in both works.

A related technique that takes the material dissimilarity into account was developed in Alves and Oshiro (2006). The difference to the present work is that Alves and Oshiro (2006) employed a distinct method to calculate the velocity factor, β_V, and the dependence of the dynamic yielding stress to strain rate was given by Cowper-Symonds constitutive relation, Eq. (8). In that study, the material parameters σ_0, q, and D of the model could be different of the prototype ones. Conversely, although the method did not rely on any data of the prototype, it required an estimation of the strain rate of the model. For complex structures it can be intricate to be calculated. In contrast, the velocity factor developed in the present work, Eq. (7), is rather simple.

The study presented by Drazetic et al. (1994) also considered the strain rate effect and distortion of material properties in the model. However, the structure response was necessary to generate the correspondence between the scaled model and the prototype.

6. CONCLUSION

As discussed in section 5, the sheet that composes the 1/4 model exhibited a quasi-static yielding stress 21.77% higher than the material of the prototype, even though they are nominally the same (low carbon steel 1006). It represented an increase in the velocity factor of 10.35% when it was calculated according to Eq. (7). The other effect studied in the present work, strain rate, contributed with 3% for β_V value, an increase of 6% in total kinetic energy. The velocity factor was calculated through Eq. (7), and relied on the material property, q, and the scaling factor, β. The prototype specimen was tested only to examine the MLT and VSG-m performance, but any data of the tests was used to determine β_V.

Even though the material did not match the requirements of the similarity theory (rigid perfectly plastic material), the VSG-m generated a considerable improvement in the results to predict the prototype behaviour when its performance is compared to the MLT, Fig. 6 and Tab. 4. The difference between the real-size structure and the MLT can be more pronounced in models with lower scaling factors or made of materials more sensitive to strain rate. The value of $\beta = 1/4$ used in the present work is rather high.

The main objective of this work was to analyse the similarity method delineated in section 2. A new set of scaling factors was developed, and they were employed to predict the prototype behaviour through the model response. It is primarily motivated by the fact that many experiments of scaled structures subjected to impact loads do not comply with the usual scaling laws. This technique is rather simple, and it can handle restrictions that the MLT is not able to overcome.

7. ACKNOWLEDGEMENTS

The authors would like to thank the Brazilian research funding FINEP for the financial support, and Mr. Caio C. F. Brasilino to his valuable help with the experiments.

8. REFERENCES

Alves, M. and Oshiro, R.E., 2006. "Scaling impacted structures when the prototype and the model are made of different materials", International Journal of Solids and Structures, Vol. 43, No. 9, pp. 2744-2760.

Baker, W.E., Westine, P.S., Dodge, F.T., 1991. "Similarity Methods in Engineering Dynamics – Theory and Practice of Scale Modeling", revised edition, Ed. Elsevier, Amsterdam; New York, 396 p.

Booth, E., Collier, D., Miles, J., 1983. "Impact scalability of plated steel structures". In: Jones, N. and Wierzbicki, T. Structural Crashworthiness, Ed. Butterworks, London, pp. 136-174.

Drazetic, P., Ravalard, Y., Dacheux, F., Marguet, B., 1994. "Applying non-direct similitude technique to the dynamic bending collapse of rectangular section tubes", International Journal of Impact Engineering, Vol. 15, No. 6, pp. 797-814.

Fox, R.W. and McDonald, A.T., 1998. "Introduction to fluids mechanics", 4th ed, Ed. John Wiley & Sons, New York, 768 p.

Gregory, L.F., 1995. "Replica model scaling for high strain-rate events", International Journal of Impact Engineering, Vol. 16, No. 4, pp. 571-583.

Hu, Y.Q., 2000. "Application of response number for dynamic plastic response of plates subjected to impulsive loading", International Journal of Pressure Vessels, Vol. 77, No. 12, pp. 711-714.

Jiang, P., Tian, C.J., Xie, R.Z., Meng, D.S., 2006. "Experimental investigation into scaling laws for conical shells struck by projectiles", International Journal of Impact Engineering, Vol. 32, No. 8, pp. 1284-1298.

Jones, N., 1997. "Structural Impact", Ed. Cambridge University Press, Cambridge, 592 p.

Johnson, W., 1972. "Impact strength of materials", Ed. Edward Arnold, London, 376 p.

Lemaitre, J. and Chaboche, J.L., 1991. "Mechanics of solids materials", Ed. Cambridge University Press, Cambridge, 584 p.

Li, Q.M. and Jones, N., 2000. "On dimensionless number for dynamic plastic response of structural members", Archive of Applied Mechanics, Vol. 70, No. 4, pp. 245-254.

Mazzariol, L.M., Calle, M.A.G., Oshiro, R.E., Alves, M., 2010. "Scaling of stiffened panels subjected to impact loading", 31 st CILAMCE, Buenos Aires.

Me-Bar, Y., 1997. "A method for scaling ballistic penetration phenomena", International Journal of Impact Engineering, Vol. 19, No. 9-10, pp. 821-829.

Murphy, G., 1950. "Similitude in engineering", Ed. The Ronald Press Company, New York, 302 p.

Neuberger, A., Peles, S., Rittel, D., 2007. "Scaling the response of circular plates subjected to large and close-range spherical explosions. Part I: Air-blast loading", International Journal of Impact Engineering, Vol. 34, No. 5, pp. 859-873.

Oshiro, R.E. and Alves, M., 2004. "Scaling impacted structures", Archive of Applied Mechanics, Vol. 74, No. 1-2, pp. 130-145.

Oshiro, R.E. and Alves, M., 2009. "Scaling of structures subject to impact loads when using a power law constitutive equation", International Journal of Solids and Structures, Vol. 46, No. 18-19, pp. 3412-3421.

Schleyer, G.K., Hsu, S.S., White, M.D., 2004. "Scaling of pulse loaded mild steel plates with different edge restraint", International Journal of Mechanical Sciences, Vol. 46, No. 9, pp. 1267-1287.

Skoglund, V.J., 1967. "Similitude – Theory and Applications", Ed. International Textbook Company, Pennsylvania, 320 p.

Snyman, I.M., 2010. "Impulse loading events and similarity scaling", Engineering Structures, Vol. 32, No. 3, pp. 886-896.

Szirtes, T., 1997. "Applied dimensional analysis and modeling", Ed. McGraw-Hill, New York, 790 p.